Molecular Thermodynamics of Asphaltene Precipitation in Reservoir Fluids

Jianzhong Wu and John M. Prausnitz
Dept. of Chemical Engineering, University of California, Berkeley, and
Chemical Sciences Division, Lawrence Berkeley National Laboratory, Berkeley, CA 94720

Abbas Firoozabadi
Reservoir Engineering Research Institute, Palo Alto, CA 94304

A previously described molecular-thermodynamic framework, based on colloid theory, is used to correlate experimental asphaltene-precipitation data at high-temperature and pressure conditions. In this framework, asphaltenes and resins are represented by pseudopure components, and all other components in a crude oil are presented by a continuous medium that affects van der Waals attractions among asphaltene and resin molecules. Model parameters are evaluated systematically from average properties of asphaltenes and resins in crude oils, and from dispersion-force properties of the oil medium. Given the composition of the medium, and asphaltene and resin concentrations, the molecular-thermodynamic model described here can be used to identify the onset of asphaltene precipitation, and the total amount of precipitation at the given operation conditions. Calculated results for the effects of oil composition and pressure on asphaltene precipitation are in good agreement with at least some experimental measurements for four reservoir fluids, including Texaco, Shell, Weyburn, and North-Sea crude oils.

Introduction

Asphaltene precipitation is a perennial problem in production and refining of crude oils. To avoid precipitation, it is useful to know the solubility of asphaltenes in petroleum liquids as a function of temperature, pressure, and liquid-phase composition. In our earlier work (Wu et al., 1998), a molecular-thermodynamic framework was developed to describe the phase behavior of asphaltene-containing fluids. In this framework, we represent asphaltenes by attractive hard spheres, resins by attractive hard-sphere chains, and all other components by a continuous medium that affects interactions between asphaltene−asphaltene, asphaltene−resin, and resin−resin pairs. We consider explicitly associations between asphaltene and asphaltene, and between asphaltene and resin. The potential of mean force between asphaltene and asphaltene, as well as that between asphaltene and resin, includes hard-sphere repulsion, van der Waals attraction, and association. Based on experimental evidence, we postulate that, while asphaltene molecules can associate themselves or with resin chains, resin chains cannot associate with themselves. Resins, when associated with asphaltenes, stabilize asphaltenes, thereby reducing their tendency to precipitate. We have shown that our molecular−thermodynamic framework can explain essentially all experimental observations for the effects of temperature, pressure, and crude-oil composition on asphaltene precipitation. In this work, we present a quantitative description of phase behavior based on the previously described framework, and we illustrate its reduction to practice: once the model parameters are fixed with a few measurements, our molecular−thermodynamic framework can predict semiquantitatively asphaltene precipitation at a variety of operating conditions.

Correspondence concerning this article should be addressed to J. M. Prausnitz.

We consider a crude oil containing asphaltenes and resins. Asphaltenes are represented by attractive hard spheres that can associate with themselves, and resins are represented by attractive hard-sphere chains that can associate with asphaltenes, but not with themselves. Asphaltene molecules and resin chains are dissolved in a continuous medium that affects dispersion-force interactions among asphaltenes and resin chains. The Helmholtz energy of the system is given by an expression based on random-phase-approximation theory (RPA) and on statistical-associated-fluid theory (SAFT) within the McMillan-Mayer description of liquid solutions. The Helmholtz energy A contains five contributions:

$$A = A^{id} + A^{hs} + A^{vdw} + A^{assoc} + A^{chain}, \tag{1}$$

where superscript *id* stands for an ideal-gas mixture of asphaltenes and resin chains at system temperature, volume, and molecular number densities; *hs* stands for the contribution from hard-sphere repulsion when resin chains are disconnected; *vdw* stands for the contribution from van der Waals (dispersion-force) attractions; *assoc* stands for the contribution from asphaltene–asphaltene and asphaltene–resin associations; and *chain* stands for the entropic contribution to A from connectivity of resin chains.

The ideal-gas contribution to the Helmholtz energy takes into account the translational kinetic energy of asphaltenes and resin chains in the solution. It is given by

$$\frac{A^{id}}{kT} = \sum_{i=A,R} N_i \ln\left(\rho_i \Lambda_i^3\right) - N_t, \tag{2}$$

where k is the Boltzmann constant; T is absolute temperature; N_A and N_R are the number of asphaltene molecules and resin chains; $N_t = N_A + N_R$ is the total number of molecules; $\rho_A = N_A/V$ and $\rho_R = N_R/V$ are, respectively, the number densities of asphaltene molecules and resin chains; V stands for volume; Λ_i stands for the thermal wavelength of molecule i for $i = A$, asphaltene molecule, and for $c = R$, resin chain. Because Λ_i depends only on temperature for a given i, it cancels in phase-equilibrium calculations.

The contribution to the Helmholtz energy from hard-sphere interactions among asphaltene and resin segments (not resin chains) is obtained from the equation of Mansoori et al. (1971):

$$\frac{A^{hs}}{kT} = N_t^s\left\{\left[\frac{\xi_2^3}{\xi_0\xi_3^2} - 1\right]\ln(1-\xi_3) + \frac{3\xi_1\xi_2}{\xi_0(1-\xi_3)} + \frac{\xi_2^3}{\xi_3\xi_0(1-\xi_3)^2}\right\}, \tag{3}$$

where N_t^s is the number of asphaltene segments plus the number of resin segments; $\xi_n = (\pi/6)\sum_{i=1}^{2}\rho_i\sigma_i^n$, $n = 0, 1, 2, 3$. When $n = 0$, ξ_0 is a density; when $n = 3$, ξ_3 is the packing fraction. Subscripts $i = 1, 2$ denote asphaltene segment (1) and resin segment (2), respectively. Because we represent asphaltene molecules by attractive hard spheres, an asphaltene segment is identical to an asphaltene molecule; thus we have $\rho_A = \rho_1$. However, because a resin chain contains several segments, $\rho_R = \rho_2/l_R$, where l_R stands for the number of segments per resin chain. The segment diameter for component i is denoted by σ_i.

The contribution to the Helmholtz energy from van der Waals attractions among asphaltene and resin segments in a medium is obtained from the RPA (Hansen and McDonald, 1986):

$$\frac{A^{vdw}}{kT} = \frac{V}{2}\sum_{i=1}^{2}\sum_{j=1}^{2}\rho_i\rho_j\frac{U_{ij}}{kT}, \tag{4}$$

where $U_{ij} = 4\pi\int_{\sigma_{ij}}^{\infty} W_{ij}^{vdw}(r) r^2\,dr$ with $\sigma_{ij} = (\sigma_i + \sigma_j)/2$. In Eq. 4, U_{ij}/V is the (mean-field) average pair-dispersion energy for all ij pairs, that is, for all pairs formed by asphaltene and resin segments in the oil medium (U_{ij} is similar to parameter a_{ij} in the van der Waals equation of state for mixtures). The potential of mean force, $W_{ij}^{vdw}(r)$, due to dispersion interaction between two segments in an oil medium is given by (Wu et al., 1998)

$$W_{ij}^{vdw}(r) = -\frac{H_{imj}}{\pi^2\rho_i^0\rho_j^0}\frac{1}{r^6}, \tag{5}$$

where ρ_i^0 is the segment number density of pure component i, that is, "pure" asphaltenes or "pure" resin segments; r is the center-to-center distance between two segments; H_{imj} is the Hamaker constant for the interaction of i with j when i and j are immersed in medium m; it is approximated by (Israelachvili, 1991):

$$H_{imj} = \left(H_i^{1/2} - H_m^{1/2}\right)\left(H_j^{1/2} - H_m^{1/2}\right), \tag{6}$$

where H_i, H_j, and H_m are the Hamaker constants of pure i, pure j, and medium m. Equations 5 and 6 indicate that the potential of mean force due to dispersion interactions depends on the Hamaker constants of asphaltene, resin, and the oil medium, as well as on the number densities of "pure" asphaltene and resin segments.

Next, we consider asphaltene–asphaltene and asphaltene–resin associations. We assume that each asphaltene molecule has N_a identical association sites, and each resin chain has only one association site. Asphaltene can associate with each other, but resin chains can only associate with asphaltenes. The Helmholtz energy due to association is given by (Chapman et al., 1990)

$$\frac{A^{\text{assoc}}}{N_t kT} = N_\alpha X_A\left(\ln x_\alpha + \frac{1-x_\alpha}{2}\right) + X_R\left(\ln x_\beta + \frac{1-x_\beta}{2}\right), \tag{7}$$

where X_A and X_R are, respectively, mole fractions of asphaltene molecules and resin chains on a medium-free basis; x_α is the fraction of association sites at asphaltene molecules that are not bonded; x_β is the fraction of association sites at resin chains that are not bonded. Fractions x_α and x_β are given by

$$x_\alpha = \left(1 + N_\alpha \rho_A \Delta^{\alpha\alpha} x_\alpha + \rho_R \Delta^{\alpha\beta} x_\beta\right)^{-1} \quad (8)$$

$$x_\beta = \left(1 + N_\alpha \rho_A \Delta^{\alpha\beta} x_\alpha\right)^{-1}, \quad (9)$$

where ρ_A, ρ_R are as before; the number densities of asphaltene molecules and resin chains in the oil medium; $\Delta^{\alpha\alpha}$, $\Delta^{\alpha\beta}$ are given by

$$\Delta^{\alpha\alpha} = g_{11}^{hs}(\sigma_{11})\left[\exp(\zeta^{\alpha\alpha}/kT) - 1\right]\sigma_{11}^3 \kappa^{\alpha\alpha} \quad (10)$$

$$\Delta^{\alpha\beta} = g_{12}^{hs}(\sigma_{12})\left[\exp(\zeta^{\alpha\beta}/kT) - 1\right]\sigma_{12}^3 \kappa^{\alpha\beta}, \quad (11)$$

where $g_{ij}^{hs}(\sigma_{ij})$ is the contact value of the pair correlation function in the hard-sphere mixture of asphaltene and resin segments given by

$$g_{ij}^{hs}(\sigma_{ij}) = \frac{1}{1-\xi_3} + \frac{3\sigma_i\sigma_j}{(\sigma_i+\sigma_j)}\frac{\xi_2}{(1-\xi_3)} + 2\left(\frac{\sigma_i\sigma_j}{\sigma_i+\sigma_j}\right)^2 \frac{\xi_2^2}{(1-\xi_3)^3}, \quad (12)$$

$\kappa^{\alpha\alpha}$ and $\kappa^{\alpha\beta}$ are parameters related to the square-well widths for the association potentials. To reduce the number of unknown parameters, we assume that they are identical constants for associations between asphaltene and asphaltene, and between asphaltene and resin chain.

Finally, the contribution to the Helmholtz energy from chain connectivity of resin segments is given by (Chapman et al., 1988):

$$\frac{A^{\text{chain}}}{kT} = N_R(1 - l_R)\ln\left[g_{22}^{hs}(\sigma_{22})\right], \quad (13)$$

where $g_{22}^{hs}(\sigma_{22})$ is the contact value of the pair correlation function between resin segments given by Eq. 12. Equation 13 takes into account the difference in hard-sphere contribution of the Helmholtz energy between hard-sphere chains and unconnected hard spheres.

Calculations presented earlier (Wu et al., 1998) showed that the above molecular-thermodynamic framework can explain essentially all observed experimental results for asphaltene precipitation in crude oils, that is, the effects of temperature, pressure, and composition. To apply this framework to asphaltene precipitation at reservoir conditions, we first need to establish a reliable method to estimate required model parameters. Because asphaltene precipitation at reservoir conditions is often accompanied by a vapor–liquid equilibrium (VLE), and because the Hamaker constant of the medium depends on its density and composition, we also need a reliable method for estimating liquid density and VLE for reservoir fluids. For this purpose, we use the volume-shifted Peng-Robinson equation of state with an appropriate C_{7^+} characterization method, as summarized in Appendix A. With VLE and liquid density from the volume-shifted Peng-Robinson equation of state, asphaltene precipitation (liquid–liquid equilibria) can be calculated using the molecular thermodynamic model.

Molecular Parameters for Asphaltene Precipitation

For quantitative applications, molecular parameters must be estimated independently or from a few experimental data for the particular system of interest. The model parameters of our model include the diameter of the asphaltene molecule (segment) σ_1 and the diameter of resin segment σ_2; the number of segments per resin chain, l_R; the Hamaker constants for "pure" asphaltene, for "pure" resin, and for the oil medium, H_A, H_R, H_m; the asphaltene–asphaltene association energy ζ_{AA}; the asphaltene–resin association energy ζ_{AR}; the number of association sites of each asphaltene molecule N_α; and the volume parameter κ in the SAFT equation. Further, to calculate the Hamaker constant between asphaltene and resin pairs in a medium, we need to know the segment densities of pure asphaltenes and pure resins. These properties are not readily obtained from typical asphaltene or crude-oil characterizations.

For phase-equilibrium calculations, we use average molecular weights and densities for pure asphaltenes and resins. As discussed by Speight (1991, 1994), the average molecular weights of asphaltenes and resin chains are about $M_A = 2{,}000$ and $M_R = 800$ Da, respectively. The mass density of a typical asphaltene is about $d_A^0 = 1200$ kg/m^3, close to that of the heaviest hydrocarbons, and the mass density of a typical resin is about $d_R^0 = 1{,}000$ kg/m^3 (Speight, 1991). From the mass densities and molecular weights, we can calculate the number densities of pure asphaltenes and resin chains.

To a good approximation, the packing fraction of pure asphaltene, defined as $\pi\rho_1\sigma_1^3/6$, lies between the minimum packing fraction of a hard-sphere solid (~ 0.55) and the highest liquid packing fraction of hard spheres (~ 0.74). Using the molecular weight of asphaltene, $M_A = 2{,}000$ Da and mass density $d_A^0 = 1{,}200$ kg/m^3, we find that the diameter of an asphaltene molecule (segment) lies in a narrow range, $1.43 < \sigma_1 < 1.58$ nm. In our calculations, we use $\sigma_1 = 1.5$ nm corresponding to about the minimum asphaltene diameter reported in the literature. Because asphaltene molecules strongly bind with themselves in most solvents, experimental measurements often tend to give the sizes of asphaltene aggregates instead of asphaltene monomers.

To our best knowledge, no size information has been published for resin chains. Because resin is a liquid at ambient conditions, its packing fraction should be less than that of a hard-sphere solid at the fluid–solid phase transition (~ 0.55). We assume that the diameter of a resin segment is about 0.5 nm, and the number of segments per chain is about 10. With these parameters, and with molecular weight of resin, $M_R =$ 800 Da and mass density $d_R^0 = 1000$ kg/m^3, the packing fraction of pure resin chain is 0.49, reasonable for a high-boiling hydrocarbon. Provided that reasonable values are used, we find that asphaltene-precipitation calculations are not sensitive to resin-chain length and resin-segment diameter.

In principle, the Hamaker constant of a fluid can be calculated from its polarizability and dielectric permittivity using

Lifschitz theory of van der Waals forces (Israelachvili, 1991). However, polarizability and dielectric permittivity are often not available for components in a heavy reservoir oil. On the other hand, the Hamaker constant of a fluid can be estimated from interactions between individual pairs of atoms or groups that constitute the fluid. It has been suggested that the Hamaker constants of hydrocarbons can be estimated from van der Waals interaction between CH_2 groups (Israelachvili, 1991):

$$H = \pi^2 B \rho_{CH_2}^2 \tag{14}$$

where B is the London dispersion constant and ρ_{CH_2} is the number density of CH_2 groups. For interaction between two CH_2 groups in vacuum, $B \approx 5 \times 10^{-78}$ Jm^6. Figure 1 shows Hamaker constants estimated by Eq. 14 and results calculated from the Lifshitz theory of van der Waals forces. The two methods agree remarkably well for normal alkanes. Using Eq. 14, we estimate the Hamaker constant of pure asphaltene $H_1 = 1.32 \cdot 10^{-19}$ J, and that for pure resin segments $H_2 = 9.06 \cdot 10^{-20}$ J. Contributions of heteroelements to the Hamaker constants of asphaltenes and resins are neglected.

In a realistic situation, the medium often contains light components such as CH_4, H_2S, CO_2, and N_2. The contributions of these components to the Hamaker constant of the medium can be estimated from polarizability α_0 and first ionization potential I. The London constants for light components are obtained from (Israelachvili, 1991)

$$B = \frac{3}{4} \frac{\alpha_0^2 I}{(4\pi\epsilon_0)^2}, \tag{15}$$

where ϵ_0 is the electric permittivity of free space ($\epsilon_0 = 8.854 \times 10^{-12}$ $C^2 \cdot J^{-1} \cdot m^{-1}$). Table 1 gives calculated London constants, α_0 and I for CH_4, H_2S, CO_2, and N_2. The London constants for CH_4 is about twice that for the CH_2 group in the liquid state. All other components in the oil medium are considered as an assembly of CH_2 groups. The overall Hamaker constant of the oil medium is obtained from

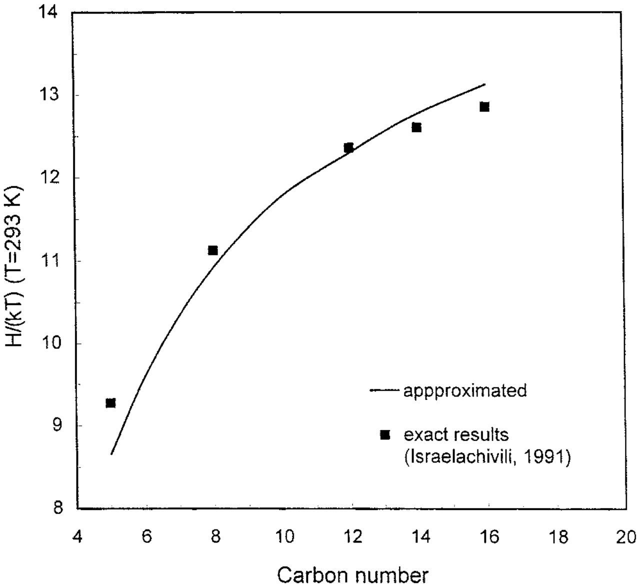

Figure 1. Hamaker constants of normal alkanes estimated from their densities.

Table 1. London Constant B, Polarizability α_0, and First Ionization Potential I for Common Light Components in Crude Oils

	α_0, Å^3	I, Ev	$B \times 10^{78}$, J·m^6
CH_4	2.59	12.51	10.1
N_2	1.74	15.58	5.67
H_2S	3.86	10.45	18.7
CO_2	2.91	13.77	14.0

α_0 and I are from *CRC Handbook of Chemistry and Physics*, 76th ed., CRC Press, New York (1995).

$$H_m = \sum_i \sum_j \pi^2 B_{ij} \rho_i \rho_j, \tag{16}$$

where $B_{ij} = \sqrt{B_i B_j}$. Here subscripts i and j refer to CH_4, H_2S, CO_2, and N_2 gases, and to the CH_2 group in the liquid state.

Because the effect of the oil medium on the potential of mean force between asphaltenes and resin segments depends only on its Hamaker constant, Eqs. 14–16 imply that the Hamaker constant of the oil medium can be determined by its density and by concentrations of light components dissolved in the medium. To verify our assertion that it is primarily the density that influences the effect of the medium on asphaltene precipitation, we have considered asphaltene precipitation in a crude oil diluted with 40 volume of solvent per volume of crude oil. More than twenty solvents are considered, including *n*-alkanes, olefins, and cycloparaffins. As shown in Figure 2, we find that the amount of asphaltene precipitation is indeed primarily determined by the solvent (medium) density. Here the medium includes the asphaltene and resin-free crude oil and the diluent. Because of the large dilution ratio, the density of solvent is essentially identical to that of the medium. The experimental data used here were reported by Mitchell and Speight (1973). Figure 2 shows that the amount of asphaltene precipitation is well correlated with the density of the hydrocarbon solvent. Because the densities of aromatics are higher than those of cycloparaffins, we expect no asphaltene precipitation when an aromatic diluent is added, as experimentally observed.

Remaining parameters are those related to the association interactions of asphaltenes and resins. As discussed by Speight (1994), the association energies between asphaltene and asphaltene, and between asphaltene and resin chains are in the range of normal hydrogen-bonding energy ($5 \sim 40$ kT_0, $T_0 = 298$ K). Also, association between asphaltene and resin is usually stronger than that between asphaltene and asphaltene. Because the properties of different asphaltene- and resin-containing crude oils are not identical, in general, the remaining parameters must be obtained by fitting to a few experimental data for asphaltene precipitation; these association parameters may vary from one crude oil to another. To

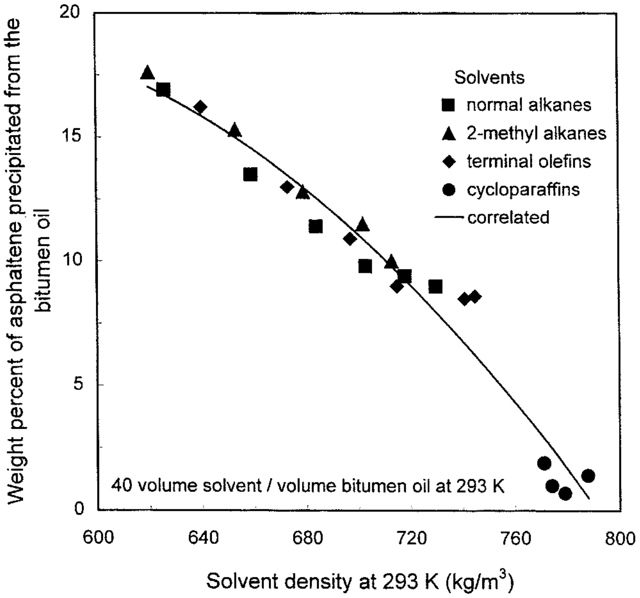

Figure 2. Correlation between asphaltene yield and solvent density.

Experimental data from Mitchell and Speight (1972).

minimize further the number of unknown parameters, the volume parameter of the SAFT equation is fixed at $\kappa = 0.05$, close to those reported by Huang and Radosz (1990) when SAFT is applied to typical associating systems, including alkanols, organic acids, and amines. Table 2 summarizes all pre-fixed parameters.

In any crude oil, there is a broad distribution of asphaltene molecular weight. In this model, we assume that asphaltene components in a crude oil can be represented by a single pseudocomponent. The average molecular weight of asphaltenes appears to be a sensitive parameter in any thermodynamic model for correlation asphaltene precipitation because it is directly related to the molar concentration of asphaltenes. Unfortunately, most experiments report only the weight percent of asphaltenes. To convert weight percent to mole concentration, an average molecular weight is required. Most earlier literature reported a high value of average molecular weight (>5000 Da) for asphaltenes because the measurements were carried out in aromatic solvents. Based on vapor-pressure osmometry experiments in pyridine solvents, Speight (1994) concluded that the average molecular weight of asphaltenes is about 2000 ± 500. However, some very recent results (after this work was completed) from gel-permeation-chromatography measurements (Pan and Firoozabadi, 1998b; Nalwaya et al., 1999; Artok et al., 1999) in CH_2Cl_2 or THF solvents give much lower (about 700 Da) number-average molecular weights. Our use of 2,000 Da is nevertheless valid because asphaltenes exist as oligomers rather than monomers in a crude oil. If a smaller average molecular weight is used, the association ability among monomers should be increased correspondingly (compared to that for a larger monomer) such that asphaltenes have a distribution of large oligomers. In addition, if the molecular weight of the monomer is reduced, the molecular size of the monomer must be reduced accordingly. Because association between asphaltene molecules is not well understood, and because asphaltenes are known to exist as large aggregates in a crude oil, it is not unreasonable to assume an effective asphaltene unit that is larger than that corresponding to a more reactive "real" monomer. After the average molecular weight of asphaltenes is fixed, there is not much room to adjust the monomer size, because both the packing fraction and the density of asphaltene do not vary much with respect to the source of crude oil or solution conditions.

Hamaker constants of asphaltene, resin, and the medium affect dispersion interactions among asphaltene and resin molecules; these parameters are not as sensitive as association parameters. As shown in Figure 2, however, as the density of the medium (solvent) increases, the dispersion interaction among asphaltene and resin molecules falls, producing a dramatic decrease in the total amount of asphaltene precipitation. Our parameters for resins are less justified than those for asphaltene. Although the parameters given in Table 2 are obtained by reasonable assumptions, it is clear that further work on the optimization of these parameters is required. Regrettably, such optimization requires a substantial database.

Asphaltene Precipitation in Crude Oils

We have calculated asphaltene precipitation equilibria for a few crude oils at high-temperature and high-pressure conditions. These crude oils include Shell oil (Hirschberg et al., 1984), Texaco oil (Burke et al., 1990), Weyburn oil (Sirvastava et al., 1995), and North-Sea oil (Fotland et al., 1997). Table 3 summarizes asphaltene and resin contents and light-component compositions of the reservoir fluids used in our calculations.

When two liquid phases coexist at equilibrium, the chemical potential for each component is the same in both phases:

$$\mu'_A = \mu''_A \tag{17}$$

$$\mu'_R = \mu''_R \tag{18}$$

where $'$ and $''$ represent two equilibrated phases. In addition, MacMillan-Mayer theory requires that the osmotic pressures for the two equilibrated phases must be equal,

$$P' = P'', \tag{19}$$

where P denotes osmotic pressure. Both chemical potentials and osmotic pressure can be obtained from Helmholtz en-

Table 2. Independently Estimated Molecular Parameters

	Asphaltene	Resin Chain
Molecular weight, Da	2,000	800
Mass density, kg/m^3	1,200	1,000
Number of segments	1	10
Segment diameter, Å	15	5
Hamaker constant, 10^{20}, J	13.2	9.06
SAFT κ-parameter	0.05	0.05

Table 3. Characterization Data for Reservoir Fluids Used in the Calculations

Texaco Reservoir				Shell Tank Oil		Weyburn Oil		North-Sea Oil		
	HCG* mol %	Oil #1 mol %	Oil #2 mol %		mol %		mol %		Sep. Oil mol %	Sep. Gas mol %
N_2	3.17	0.57	0.51	C_1	0.1	N_2	0.96	N_2	0	2.357
CO_2	17.76	2.46	1.42	C_2	0.48	CO_2	0.58	CO_2	0	0.426
C_1	30.33	36.37	6.04	C_3	2.05	H_2S	0.3	C_1	8.365	67.496
C_2	26.92	3.47	7.00	i-C_4	0.88	C_1	4.49	C_2	4.848	12.793
C_3	13.09	4.05	6.86	n-C_4	3.16	C_2	2.99	C_3	7.888	9.733
i-C_4	1.26	0.59	0.83	i-C_5	1.93	C_3	4.75	i-C_4	1.486	1.215
n-C_4	4.66	1.34	3.35	n-C_5	2.58	i-C_4	0.81	n-C_4	5.586	3.027
i-C_5	0.77	0.74	0.70	C_6	4.32	n-C_4	1.92	i-C_5	2.201	0.815
n-C_5	1.26	0.83	3.46	C_{7^+}	84.5	i-C_5	1.27	n-C_5	3.263	0.761
C_6	0.78	1.62	3.16			n-C_5	2.19	C_6	4.53	0.619
C_{7^+}	0.00	47.96	66.67			C_{6^+}	79.74	C_{7^+}	61.833	0.758
M_{C^+}, Da		329	281		250	(C_{6^+})	230		218	
C_{7^+} density, g/ml		0.96	0.90		0.96	(C_{6^+})	0.870		0.83	
wt. % asphaltene**		16.8	9		3.9		4.7		0.9	
wt. % resin		21.5	12.25		14.1		8.51		2.8	

*HCG refers to hydrocarbon gas.
**Measured according to the standard ASTM method.

ergy A as given in Eq. 1

$$\mu_A = \left(\frac{\partial A}{\partial N_A} \right)_{T,V,N_R} \tag{20}$$

$$\mu_R = \left(\frac{\partial A}{\partial N_R} \right)_{T,V,N_A} \tag{21}$$

$$P = -\left(\frac{\partial A}{\partial V} \right)_{T,N_A,N_R}, \tag{22}$$

where N_A and N_R are the number of asphaltene molecules and resin chains, respectively; V is total volume and T is temperature. Phase equilibria are calculated using Eqs. 17–19 coupled with three material-balance equations:

$$N_A' + N_A'' = N_A^0 \tag{23}$$

$$N_R' + N_R'' = N_R^0 \tag{24}$$

$$N_m' + N_m'' = N_m^0, \tag{25}$$

where superscript 0 indicates before phase separation; N_m is the total number of medium molecules. Because it is difficult to predict accurately the density of a heavy crude oil, and the change in total volume usually is small after phase separation, we replace Eq. 25 with $V' + V'' = V^0$, where V' and V'' are total volumes in phase $'$ and phase $''$, respectively; V^0 is the total volume before phase separation. Given temperature, total volume, and the total numbers of asphaltene and resin molecules, from Eqs. 17–19, Eqs. 23 and 24, and $V' + V'' = V^0$, we can obtain N_A', N_R', N_A'', N_R'', V', and V'' using the Brandt algorithm for a set of nonlinear equations with initial guesses provided by phase-stability analysis (Michelsen, 1982; Wasylkiewicz et al., 1996).

The onset of asphaltene precipitation is found through global-phase-stability analysis using the Gibbs-tangent-plane method (Wasylkiewicz et al., 1996). Either simulated annealing or simplex algorithm is used to search for the global minimum of the tangent-plane distance (Pan and Firoozabadi, 1998a).

When an asphaltene-containing crude oil is in contact with a gas phase, we need to find the composition of the oil medium, as well as the asphaltene and resin concentrations of the crude-oil phase from the vapor–liquid equilibrium. For this purpose, we use the volume-shifted PREOS. Binary parameters k_{ij} for interactions among the light components are obtained from Katz and Firoozabadi (1978). For interactions among heavy hydrocarbons, we use the Chueh-Prausnitz correlation (1967):

$$k_{ij} = 1 - \left(\frac{2 V_{c_i}^{1/6} V_{c_j}^{1/6}}{V_{c_i}^{1/3} + V_{c_j}^{1/3}} \right)^{\theta}, \tag{26}$$

where V_c is critical volume estimated from Twu's correlation (1984); θ is a parameter independent of the heavy–heavy *ij* pair, fixed by one experimental bubble-point pressure measurement.

Texaco crude oils

Burke et al. (1990) reported experimental asphaltene-precipitation data for mixtures containing crude oil and scrubber gas (85 mol % CO_2 + 15 mol % H_2S), and for mixtures containing crude oil and hydrocarbon gas. Burke and coworkers were concerned with the effect of pressure and composition on precipitate formation at elevated temperatures.

The crude oils investigated in these experiments are in equilibrium with a gas phase. To find the composition of asphaltene-containing crude oil, we first apply the volume-shifted Peng-Robinson equation of state for vapor–liquid equilibrium calculations. Figure 3 illustrates predicted and measured saturation pressures for mixtures of Texaco oil #2 and hydrocarbon gas at 376.6 K. For this mixture, the θ-parameter in Eq. 26 is 0.66, obtained from the experimental bubble-point pressure of this oil at reservoir conditions.

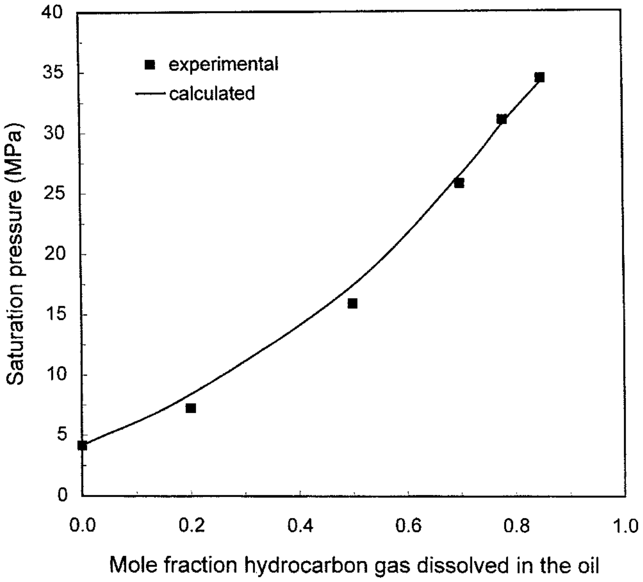

Figure 3. Saturation pressures for mixtures of Texaco Oil #2 and hydrocarbon gas at 376.6 K.

Agreement between calculated and experimental results for the saturation pressure is excellent.

To calculate asphaltene precipitation of the crude-oil phase at various temperatures and oil compositions, we use estimated association parameters $N_a = 6$, $\zeta_{AA}/kT_0 = 5$, and $\zeta_{AR}/kT_0 = 10$ ($T_0 = 298$ K), as discussed previously (Wu et al., 1998). Because the experimental data scatter widely, there is no advantage in further refinement of these molecular parameters. However, because the resin contents are not reported for the Texaco crude oils used here, we fix the resin content by adjusting the calculated amount of asphaltene precipitation with one experimental measurement for each crude oil. The "fitted" resin content may not be identical to that actually present in the crude oil. The fitted weight percents of resins of two Texaco oils are also listed in Table 3.

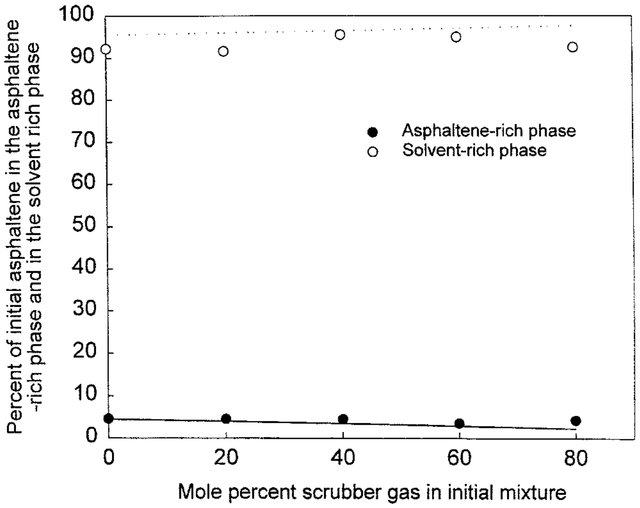

Figure 4. Asphaltene precipitation for Texaco Oil #1 in contact with scrubber gas.

$T = 373$ K, $P = 20.9$ MPa; points are measurements by Burke et al. (1990); lines are calculated.

Figure 4 shows asphaltene precipitation from mixtures of Texaco oil #1 and a scrubber gas at 373 K and 20.9 MPa. At the conditions shown in this plot, the applied pressure is lower than the saturation pressures of the mixtures; therefore, the crude oil is in contact with a gas phase. Figure 4 presents the amount of asphaltene in both the asphaltene-rich liquid phase and in the solvent-rich phase after asphaltene precipitation. Due to experimental uncertainties, measured amounts of asphaltenes in the two equilibrated liquid phases do not satisfy material balances. Both experiment and calculated results show that the amount of asphaltene precipitated falls slightly as the overall concentration of the scrubber gas rises. The decline in the amount of asphaltene precipitation is because the liquid density of the oil medium increases as more scrubber gas dissolves in the crude oil at the prevailing temperature and pressure. Our calculated results agree reasonably well with the experimental measurements.

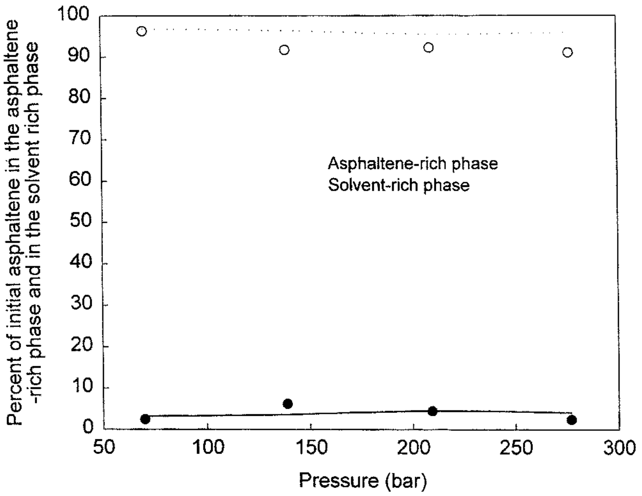

Figure 5. Effect of pressure on asphaltene precipitation for Texaco oil #1 at 373 K.

Saturation pressure = 20.3 MPa; points are measurements by Burke et al. (1990); lines are calculated.

Figure 5 shows the effect of pressure on asphaltene precipitation for the same crude oil as that discussed in Figure 4. Because we have fixed all model parameters and resin content, no additional adjustable parameters are used in these calculations. The saturation pressure of the crude oil is about 200 bar. Both experiment and our theory show a weak nonmonotonic pressure effect on the amount of asphaltene precipitation. This nonmonotonic effect is related to the saturation pressure of the mixture. When the applied pressure is lower than the saturation pressure of the mixture, an increase in pressure dissolves more gas, causing more asphaltene precipitation; on the other hand, when the pressure is higher than the saturation pressure, the density of the medium increases with applied pressure. The amount of asphaltene precipitation decreases as the density of the medium rises. Our calculations agree reasonably well with measurements over the pressure interval studied in the experiments. Figures 4 and 5 suggest that, once model parameters are fixed using

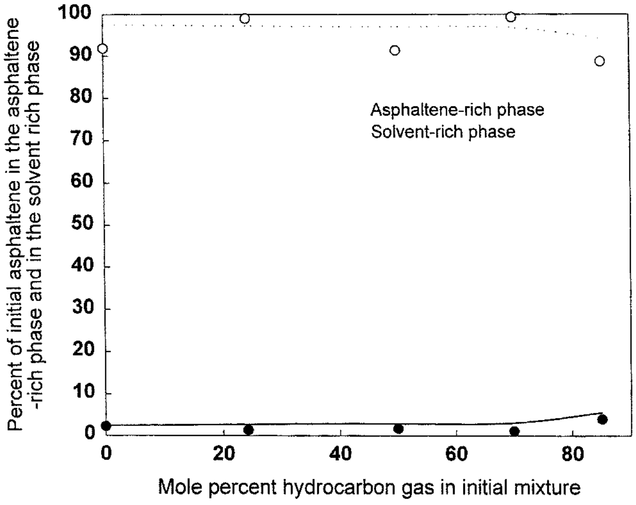

Figure 6. Asphaltene precipitation in Texaco Oil #2 by adding hydrocarbon gas at 376.6 K and 3.55 MPa.

All mixtures are below saturation pressure; points are measurements by Burke et al. (1990); lines are calculated.

some experimental data at a fixed condition, our framework can predict the amount of asphaltene precipitation at other conditions.

Figure 6 presents predicted and measured percent of asphaltene precipitation for mixtures of Texaco oil #2 and hydrocarbon gas at a given temperature and pressure. The composition of the hydrocarbon gas is also given in Table 3. The same set of model parameters is used for this oil; the resin content for this crude oil is again fixed using one experimental measurement for asphaltene precipitation. When the applied pressure is below the saturation pressures of the oil–gas mixtures, the amount of asphaltene precipitation is insensitive to the overall concentration of the hydrocarbon gas, as indicated both by calculation and by experiment. However, more asphaltenes are precipitated at very high (> 70%) hydrocarbon–gas content, as shown by calculation and by experiment. Different from the effect of scrubber gas on asphaltene precipitation (as shown in Figure 4), the density of the oil medium decreases monotonically as more hydrocarbon gas dissolves in the crude oil.

Shell tank oil

Hirschberg et al. (1984) measured the pressure at the onset of asphaltene precipitation for a Shell crude oil in contact with propane. At a given temperature, propane solubility increases with pressure, leading to asphaltene precipitation. In this calculation, we first compute the solubility of propane and the liquid density of tank oil #1. We use the volume-shifted Peng-Robinson equation of state with $k_{ij} = 0$ (where i and j refer to heavy components) because no measured bubble-point pressure is available. Then, our molecular–thermodynamic model is used to calculate the pressure at the onset of asphaltene precipitation. The concentration of resin is obtained from the content of asphalt that is understood to be the combination of asphaltene and resin. The onset pressure was determined by tangent-plane stability analysis of the system (Pan and Firoozabadi, 1998a). Figure 7 shows calculated and measured pressures at the onset of asphaltene precipitation for tank oil #1 in contact with propane. In this calculation, the number of association sites per asphaltene molecule is again equal to 6, but association energy parameters are obtained by fitting to the experimental onset-pressure data, $\zeta_{AA}/kT_0 = 5.26$ and $\zeta_{AR}/kT_0 = 7.92$, where $T_0 = 298$ K. The same set of parameters was then used to predict the onset of asphaltene precipitation for a mixture of tank oil #1 and normal decane in contact with propane at different temperatures. Figure 7 also shows predicted and measured pressures at the onset of asphaltene precipitation for the mixture of tank oil #1 and normal decane in contact with propane. For this Shell tank oil, agreement between predicted and experimental results is reasonably good. In this example, several experimental points are neglected in Figure 7 because one point is a duplicate, and because at low temperature, wax precipitation was expected as indicated by the original authors.

Weyburn reservoir oil

Sirvastava et al. (1995) have investigated the effect of a CO_2-miscible displacement process on asphaltene precipitation for Weyburn reservoir oils. In the experiments, different amounts of CO_2 and Weyburn reservoir fluid were mixed by application of high pressure. After precipitation equilibrium, the amount of asphaltene precipitated was measured by quick release of the applied pressure; Sirvastava et al. (1995) assumed that asphaltenes do not redissolve during the quick pressure-release process.

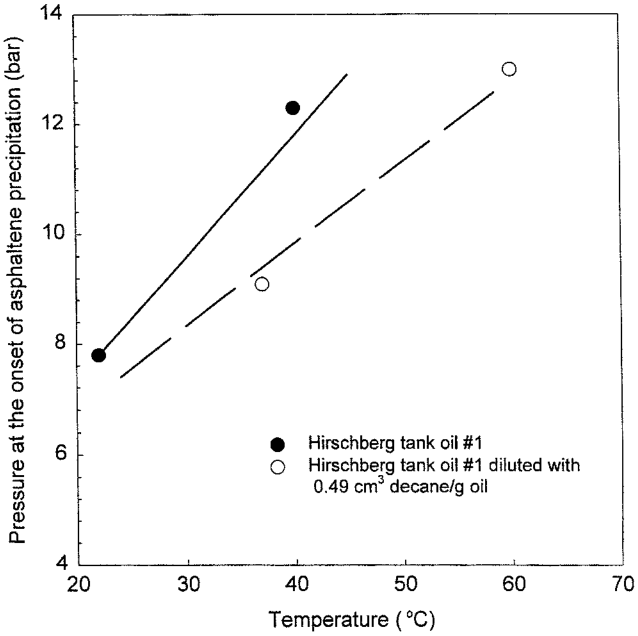

Figure 7. Effect of temperature on the pressure at onset of asphaltene precipitation by injection of propane for two Shell reservoir fluids.

Points are experimental data by Hirschberg et al. (1984); lines are calculated.

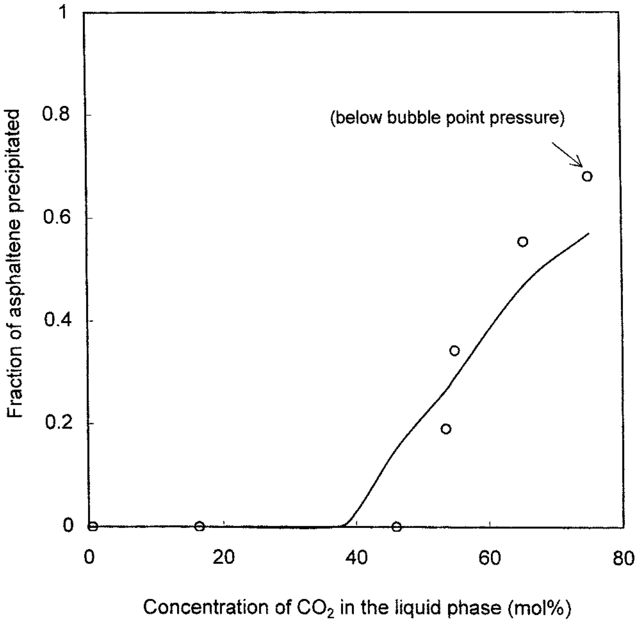

Figure 8. Effect of CO_2 injection on asphaltene precipitation for Weyburn oil at 16 MPa and 332 K.

Points are measurements by Sirvastava et al. (1995); line is calculated.

When pressure is lower than the saturation pressure, CO_2 solubility is calculated from the volume-shifted Peng-Robinson equation of state with $\theta = 2.1$ and $k_{ij} = 0.095$ for interactions between CO_2 and heavy components. Here k_{ij} and θ are obtained by fitting to measured saturation pressures of this crude oil at various temperatures. Figure 8 shows calculated and measured fractions of asphaltene precipitated at different CO_2 concentrations. In this calculation, we find that three association sites per asphaltene molecule gives the best fit of experimental results. Associated energy parameters $\zeta_{AA}/kT_0 = 12.5$ and $\zeta_{AR}/kT_0 = 9.77$ ($T_0 = 298$ K) are obtained by fitting the experimental asphaltene-precipitation data. From the volume-shifted Peng-Robinson equation of state, we find that the liquid density of the oil medium increases as more CO_2 dissolves in the crude oil. Both experiment and calculation indicate that the solubility of asphaltene in the oil declines as the content of CO_2 in the crude oil rises. If any standard solubility model were used for this example, an increase in asphaltene precipitation with rising CO_2 concentration would be expected because, as CO_2 concentration rises, the solubility parameter of the medium becomes closer to that of asphaltene. Our calculations, in agreement with experiment, show the opposite trend that follows from enhanced resin solubility in the medium. Because resin now is "more comfortable" in the medium, the tendency of resin to associate with asphaltene declines. As a result, asphaltene is destabilized and precipitates.

North-Sea crude oil

Fotland et al. (1997) investigated the effect of oil composition on the onset pressure of asphaltene precipitation for different North-Sea crude oil mixtures, made from mixing various ratios of separator oil and separator gas. Separator oil and separator gas are, respectively, the liquid and gas fractions of the reservoir oil flashed at ambient conditions. For the crude oil used here, the average C_{7^+} mass density that is used in our C_{7^+} characterization is not reported in the oil-characterization data. Thus, we first estimated the average C_{7^+} mass density by adjusting the reported density of the separator oil at 20 MPa and 365 K using the volume-shifted Peng-Robinson equation of state. Parameter θ of Eq. 26 was set at 1.42, based on the measured bubble-point pressure for the reservoir oil. Figure 9 compares predicted and measured saturation pressures and liquid densities for mixtures of the North-Sea separator oil and separator gas at 365 K. The liquid densities were not measured at the saturation pressure; instead, they were measured at constant pressure (320 bar), higher than the saturation pressures of all the mixtures. As found in other examples, the volume-shifted Peng-Robinson equation of state provides reliable predictions for liquid densities. The volume-shifted equation does not affect calculation of the saturation pressure.

Figure 10 shows the pressure at the onset of asphaltene precipitation as a function of the separator-gas concentration for the North-Sea crude oil at 365 K. We find that three association sites for each asphaltene molecule gives the best fit of experimental results for this oil. The association-energy parameters for asphaltene-asphaltene and for asphaltene-resin, $\zeta_{AA}/kT_0 = 8.35$ and $\zeta_{AR}/kT_0 = 7.49$ ($T_0 = 298$ K) are obtained by fitting the experimental data of asphaltene precipitation. As more separator gas dissolves in the crude oil, the Hamaker constant of the medium declines, leading to additional attraction between asphaltene molecules. As a result, the onset pressure increases nearly linearly with the mole fraction of separator gas in the oil.

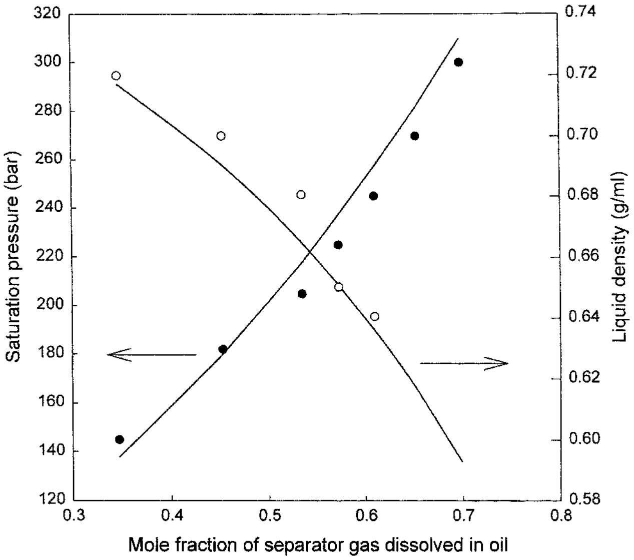

Figure 9. Calculated and measured saturation pressure, and density of mixtures of separator oil and separator gas of the North-Sea oil at 365 K.

Points are experimental data by Fotland et al. (1997); lines are calculated.

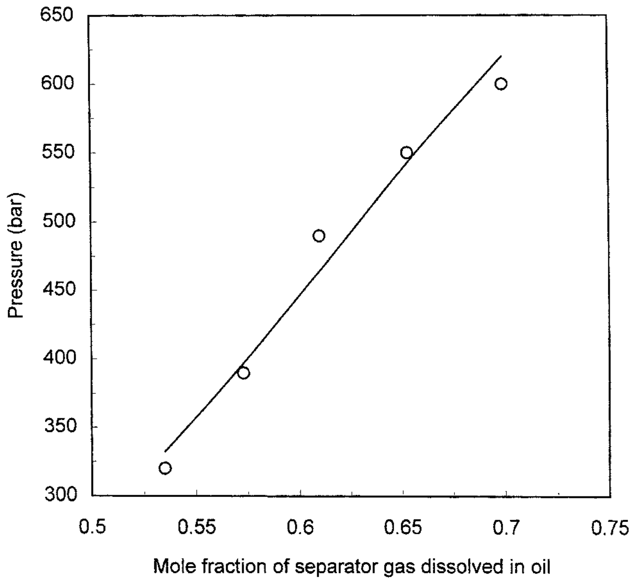

Figure 10. Calculated and experimental pressure at onset of asphaltene precipitation for North-Sea oils at 365 K.

Points are experimental data by Fotland et al. (1997); line is calculated.

Fotland et al. also reported experimental data on asphaltene precipitation for the same crude oil at 333 K. They found that temperature has essentially no effect on the pressure at the onset of asphaltene precipitation, and on the bubble-point pressure of the crude oil. It is difficult for us to interpret these results. Our model predicts that the onset pressure is sensitive to temperature changes, because a change in temperature not only affects interactions among asphaltenes and resins, but also changes the equilibrium composition of the asphaltene-containing liquid phase.

Conclusions

The effect of the oil medium on asphaltene precipitation is determined only by its Hamaker constant as obtained from the oil's density and from the concentration of light components in the oil. At reservoir conditions when the crude oil is in equilibrium with light-component gases, the properties of the medium, and the contents of asphaltene and resin in the oil phase can be reliably calculated using the volume-shifted PREOS with an appropriate C_{7+} characterization procedure and with suitable binary interaction parameters. In general, because the asphaltene content in the oil is not large, asphaltene precipitation does not significantly affect oil-vapor equilibria.

The molecular−thermodynamic model discussed here has been tested with experimental data for a few reservoir fluids to describe the effects of pressure and oil composition on asphaltene precipitation. This model can be applied to identify (1) the operation conditions at the onset of asphaltene precipitation, and (2) the amount of precipitation under various reservoir conditions. Most parameters in our model can be estimated independently from average properties of asphaltenes and resins. The parameters related to association interactions, N_a, ζ_{AA}, and ζ_{AR}, are confined within physically meaningful lower and upper limits. However, because calculated results are often sensitive to these parameters, and because asphaltenes and resins in crude oils differ from one crude oil to another, in typical cases, they must be correlated with some experimental data for the particular crude oil of interest. For the North Sea crude oil, the effect of temperature requires further study to achieve clarification.

Acknowledgments

This work was supported, in part, by the Director, Office of Energy Research, Office of Basic Energy Sciences, Chemical Sciences Division of the U.S. Department of Energy under Contract No. DE-AC03-76SF00098. For initial support, we are grateful to the University of California Energy Institute.

Literature Cited

Alexander, G. L., A. L. Creagh, and J. M. Prausnitz, "Phase Equilibria for High-Boiling Fossil-Fuel Distillates. 1. Characterization," *Ind. Eng. Chem. Fundam.*, **24**, 301 (1985).

Artok, L., Y. Su, Y. Hirose, M. Hosokawa, S. Murata, and M. Nomura, "Structure and Reactivity of Petroleum-Derived Asphaltene," *Energy Fuels*, **13**, 287 (1999).

Burke, N. E., R. E. Hobbs, and S. F. Kashou, "Measurement and Modeling of Asphaltene Precipitation," *J. Pet. Technol.*, **42**, 1440 (1990).

Chapman, W. G., G. Jackson, and K. E. Gubbins, "Phase Equilibria of Associating Fluids, Chain Molecules with Multiple Bonding Sites," *Mol. Phys.*, **65**, 1057 (1988).

Chapman, W. G., K. E. Gubbins, G. Jackson, and M. Radosz, "New Reference Equation of State for Associating Liquids," *Ind. Eng. Chem. Res.*, **29**, 1709 (1990).

Chueh, P. L., and J. M. Prausnitz, "Vapor-Liquid Equiibria at High Pressures: Calculation of Partial Molar Volume in Non-Polar Liquid Mixtures," *AIChE J.*, **13**, 1107 (1967).

Cotterman, R. L., and J. M. Prausnitz, "Flash Calculations for Continuous or Semi-Continuous Mixtures using Equation of State," *Ind. Eng. Chem. Process Des. Dev.*, **24**, 434 (1985).

Fotland, P., H. Anfinsen, H. Foerdedal, and H. P. Hjermstad, "The Phase Diagrams of Asphaltenes: Experimental Technique, Results and Modeling on Some North Sea Crude Oils," Symposium on the Chemistry of the Asphaltene and Related Substances, Cancun, Mexico (1997).

Hansen, J. P., and I. R. McDonald, *Theory of Simple Liquids*, 2nd ed., Academic Press, San Diego (1986).

Hirschberg, A., L. N. J. de Jong, B. A. Schipper, and J. G. Meyers, "Influence of Temperature and Pressure on Asphaltene Flocculation," *SPE J.*, 283 (1984).

Hong, S. G, K. A. Green, and K. D. Luks, "Solubility and Volumetric Behavior of Methane and Carbon Dioxide Plus C_{7+} Pseudo-components of an Oil," *Fluid Phase Equilibria*, **95**, 267 (1994).

Huang, S. H., and M. Radosz, "Equation of State for Small, Large, Polydisperse and Associating Molecules," *Ind. Eng. Chem. Res.*, **29**, 2284 (1990).

Israelachvili, J., *Intermolecular & Surface Forces*, Academic Press, London (1991).

Katz, D. L., and A. Firoozabadi, "Predicting Phase Behavior of Condensate/Crude-Oil Systems Using Methane Interaction Coefficients," *J. Pet. Technol.*, 1649 (1978).

Kokal, S. L., and S. G. Sayegh, "Gas-Saturated Bitumen Density Predictions Using the Volume Translated Peng-Robinson Equation of State," *J. Can. Pet. Technol.*, **29**, 77 (1990).

Mansoori, G. A., N. F. Carnahan, K. E. Starling, and T. W. Leland, "Equilibrium Thermodynamic Properties of the Mixture of Hard Spheres," *J. Chem. Phys.*, **54**, 1523 (1971).

Michelsen, M. L., "The Isothermal Flash Problem. I. Stability," *Fluid Phase Equilibria*, **9**, 1 (1982).

Mitchell, D. L., and J. G. Speight, "The Solubility of Asphaltenes in Hydrocarbon Solvents," *Fuel*, **53**, 149 (1973).

Nalwaya, V., V. Tangtayakom, P. Piumsomboon, and S. Fogler, “Studies on Asphaltenes Through Analysis of Polar Fractions,” *Ind. Eng. Chem. Res.*, **38**, 964 (1999).
Pan, H. Q., and A. Firoozabadi, “Complex Multiphase Equilibrium Calculations by Direct Minimization of Gibbs Free Energy by Use of Simulated Annealing,” *SPE Reservoir Eval. Eng.*, 36 (1998a).
Pan, H. Q., and A. Firoozabadi, “Thermodynamic Micellization Model for Asphaltene Aggregation and Precipitation in Petroleum Fluids,” *SPE Prod. Facil.*, **13**, 118 (1998b).
Peneloux, A., E. Rauzy, and R. Freze, “A Consistent Correlation for Redlich-Kwong-Soave Volumes,” *Fluid Phase Equilibria*, **8**, 7 (1982).
Peng, D. Y., and D. B. Robinson, “A New Two-Constant Equation of State,” *Ind. Eng. Chem. Fundam.*, **15**, 59 (1976).
Rackett, H. G., “Equation of State for Saturated Liquid,” *J. Chem. Eng. Data*, **15**, 514 (1970).
Reid, R. C., J. M. Prausnitz, and B. E. Poling, *Properties of Gases and Liquids*, 4th ed., McGraw-Hill, New York (1986).
Schreiber, D. R., and K. S. Pitzer, “Equation of State in the Acentric Factor System,” *Fluid Phase Equilibria*, **46**, 113 (1989).
Sirvastava, R. K., S. S. Hung, S. G. Dyer, and F. M. Mourits, “Quantification of Asphaltene Flocculation During Miscible CO_2 Flooding in the Weyburn Reservoir,” *J. Can. Pet. Technol.*, **34**, 31 (1995).
Speight, J. G., *The Chemistry and Technology of Petroleum*, Dekker, New York (1991).
Speight, J. G., “The Molecular Nature of Petroleum Asphaltenes,” *Arab. J. Sci. Eng.*, **19**, 335 (1994).
Twu, C. H., “An Internally Consistent Correlation for Predicting the Critical Properties and Molecular Weights of Petroleum and Coal-Tar Liquids,” *Fluid Phase Equilibria*, **16**, 137 (1984).
Wasylkiewicz, S. K., L. N. Sridhar, M. F. Doherty, and M. F. Malone, “Global Stability Analysis and Calculation of Liquid-Liquid Equilibrium in Multicomponent Mixtures,” *Ind. Eng. Chem. Res.*, **35**, 1395 (1996).
Whitson, C. H., T. F. Anderson, and I. Soreide, “Application of the Γ-Distribution Model to Molecular Weight and Boiling Point Data for Petroleum Fractions,” *Chem. Eng. Commun.*, **96**, 259 (1990).
Wu, J., J. M. Prausnitz, and A. Firoozabadi, “Molecular Thermodynamic Framework for Asphaltene-Oil Equilibria,” *AIChE J.*, **44**, 1188 (1998).

Appendix A: Vapor-Liquid Equilibria (VLE) and Liquid-Density Calculations Using the Volume-Shifted Peng-Robinson Equation of State (PREOS)

We use the PREOS (Peng and Robinson, 1976) to calculate VLE of reservoir fluids. To include heavy hydrocarbons, we describe a C_{7+} characterization procedure for the heavy end of a crude oil in Appendix B. With suitable binary interaction parameters (k_{ij}) and reasonable critical properties of C_{7+} pseudocomponents, the PREOS provides a good description of vapor−liquid equilibria for reservoir fluids.

For liquid-density calculations, Peneloux et al. (1982) proposed the volume-shifted equation-of-state method. They assume that for a pure component at a temperature below its critical point, the difference between the experimental liquid molar volume and that predicted by the PREOS is independent of pressure. This difference can be estimated at saturated conditions using Rackett’s equation (Rackett, 1970). At temperatures exceeding critical, the volume offset depends only on the critical compressibility factor. The liquid molar volume at an arbitrary pressure and temperature is obtained by making a correction to that calculated from the PREOS by a volume-offset calculated at the saturation pressure. For pure components at saturation conditions, the volume-shifted method gives the same results as those of Rackett’s equation. For mixtures, the overall shifted-volume equation is obtained by linear combination of the shifts for pure components. The volume-shifted method has been successfully applied to calculate the densities of gas-saturated bitumen (Kokal and Sayegh, 1990).

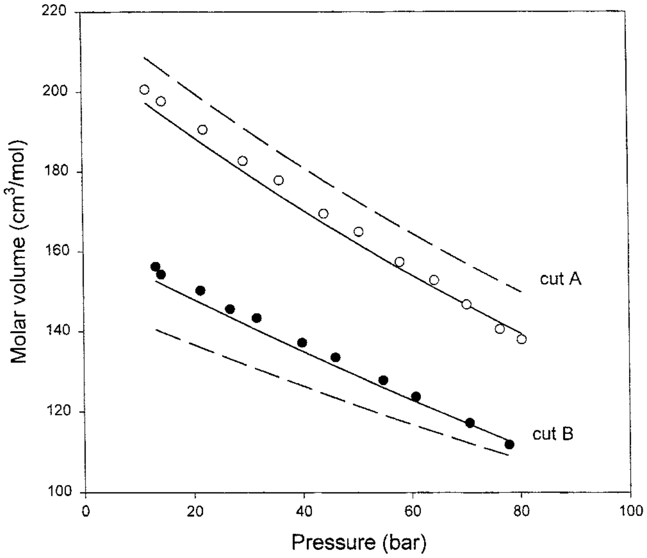

Figure A1. Comparison between volume-shifted and original PREOS for prediction of liquid molar volume of two reservoir fluids (Cut A and Cut B) at 360.9 K.

Solid lines are calculated using the volume-shifted PREOS; dashed lines are calculated using the original PREOS; points are experimental data by Hong et al. (1994).

Our application of the volume-shifted PREOS is different from that of Kokal and Sayegh (1990) for supercritical components. We calculate the volume-offset of a supercritical component by comparison with molar volumes obtained from the Schreiber-Pitzer equation (1989) at system pressure and temperature. Further, because the Rackett constant is often unavailable, especially for pseudocomponents, we calculate the Rackett constant from a single measured liquid density. For a discrete component of a crude oil, the required experimental liquid density is available at ambient conditions. For a pseudocomponent, the required single liquid density is provided by our C_{7+} characterization procedure, as discussed in Appendix B.

To illustrate, Figure A1 shows calculated and observed liquid molar volumes for two crude oils at saturation conditions. Experimental data are from Hong et al. (1994). Compared with the original PREOS, the improvement of the volume-shifted method is significant. As pointed out by Peneloux (1982), the volume-shifted method does not affect VLE calculations provided that the volume correction is applied to both liquid and vapor phases.

Appendix B: C_{7+} Characterization Method

Heptane-plus (C_{7+}) fraction refers to the components of a reservoir fluid with molecular weight or normal boiling point higher than those for *n*-hexane. Typically, C_{7+} is a complex mixture of heavy paraffins, naphthenes, and aromatics. Characterization of the C_{7+} fraction is important for calculation of phase equilibria of reservoir fluids. The C_{7+} characterization for a heavy crude oil should be based on experimental measurements from distillation or chromatographic fractionation (Alexander et al., 1985). Unfortunately, such detailed information is generally not available in the literature for asphaltene-containing mixtures. Some methods characterize a C_{7+} fraction based on molecular weight or boiling-point temperature; the C_{7+} fraction is represented by a set of pseudocomponents or by a continuous distribution function (Whitson et al., 1990, and references therein). The advantage of a traditional method is that it can represent reasonably well one particular property of the C_{7+} fraction (such as molecular-weight distribution), but it usually provides no information for other properties of practical interest (such as boiling-point temperature or density). As a result, when a cubic equation of state is used to describe the phase behavior of a reservoir fluid, the equation-of-state parameters are estimated using empirical correlations based only on one property. Subsequent calculations could be unreliable because components having one identical property may differ significantly in other properties.

The need to include both molecular-weight and density information was shown over 20 years ago by Katz and Firoozabadi (1978). Here we describe an alternative method to characterize C_{7+} fractions.

First, a C_{7+} fraction is divided into a set of pseudocomponents based on known average molecular weight and on an assumed variance; here the molecular weight of the C_{7+} fraction is represented by a Γ-distribution function, and the Gaussian quadrature method is used to convert the continuous distribution to obtain pseudocomponents (Cotterman and Prausnitz, 1985). Then the density of each pseudocomponent at ambient conditions is calculated from a correlation between the density and molecular weight. Our C_{7+} characterization method requires average and variance of molecular-weight distribution, and average density at ambient conditions. If an experimental variance is not available, we use 700 for a typical crude oil. Six quadrature points are used in most of our calculations. In general, VLE calculations are not sensitive to the variance and number of quadrature points. (However, dew point calculations are sensitive to the distribution of very heavy components.) This new procedure represents each pseudocomponent, with two properties, molecular weight and liquid density, at ambient conditions.

Table B1. Molecular Weight (MW) and Density (d) of C_7 Hydrocarbons

Hydrocarbon	T^* K	MW Da	$d \times 10^{-3}$ kg/m^3
Toluene	293	92.141	0.867
c-Heptane	293	98.189	0.81
1,2-Dimethylcyclopentane, cis	289	98.189	0.777
1,2-Dimethylcyclopenane, trans	289	98.189	0.756
Ethylcyclopentane	289	98.189	0.771
Methylcyclohexane	289	98.189	0.774
1-Heptene	293	98.189	0.697
2,3,3-Trimethyl-1-butene	293	98.189	0.705
n-Heptane	293	100.205	0.684
2-Methylhexane	293	100.205	0.679
3-Methylhexane	293	100.205	0.687
2,2-Dimethylhexane	293	100.205	0.674
2,3-Dimethylhexane	293	100.205	0.695
2,4-Dimethylhexane	293	100.205	0.673
3,3-Dimethylhexane	293	100.205	0.693
3-Ethylpentane	293	100.205	0.698
2,3,3-Trimethylbutane	293	100.205	0.69
Average	292.1	98.90	0.73

*The density is measured at temperature T and atmospheric pressure.

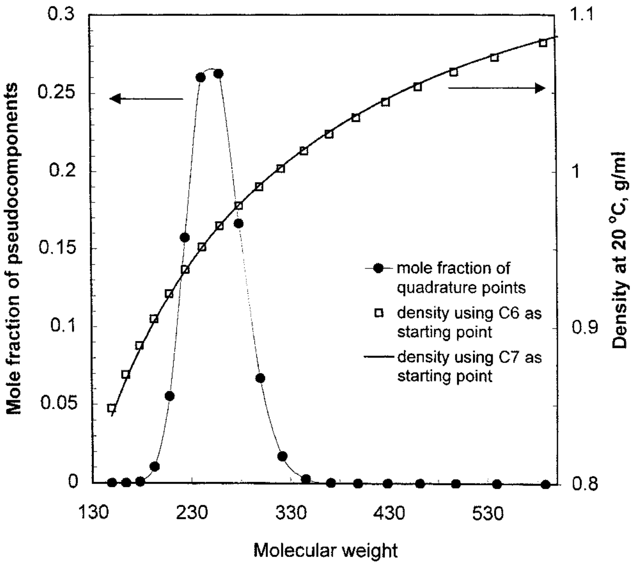

Figure B1. Molecular weights and densities of the Gaussian-quadrature points for a C_{7+} fraction in crude oil.

For this fraction, the average molecular weight = 253 Da and the average mass density = 960 kg/m^3; the calculation uses 20 quadrature points.

The correlation between density at ambient conditions, d_i, (g/mL) and molecular weight M_i (g/mol) of a C_{7+} pseudocomponent is empirically represented by

$$\frac{1}{d_i} = \frac{1}{1.2} + \frac{c_1}{M_i} + \frac{c_2}{M_i^2}, \tag{B1}$$

where c_1 and c_2 are calculated from the mole fraction of each pseudocomponent, x_i, from minimum and average molecular weights M_0 and $\overline{M}$ of the C_{7+} fraction, and from minimum and average densities d_0 and $\overline{d}$ of the C_{7+} fraction,

$$c_1 = \frac{\overline{M}\left(\frac{1}{\overline{d}} - \frac{1}{1.2}\right) - M_0^2\left(\frac{1}{d_0} - \frac{1}{1.2}\right)\sum_i \frac{x_i}{M_i}}{1 - M_0 \sum_i \frac{x_i}{M_i}} \tag{B2}$$

$$c_2 = M_0 \frac{M_0\left(\frac{1}{d_0} - \frac{1}{1.2}\right) - \overline{M}\left(\frac{1}{\overline{d}} - \frac{1}{1.2}\right)}{1 - M_0 \sum_i \frac{x_i}{M_i}}. \tag{B3}$$

In deriving Eq. A1, we assume that the maximum density of a hydrocarbon component in the C_{7+} fraction at ambient conditions is 1.2 g/mL. M_0 and d_0 are assumed to be the same as those averages of typical C_7 components given in Table B1, $d_0 = 0.73$ g/mL, $M_0 = 98.9$ g/mol.

The ambient-condition densities of C_{7^+} pseudocomponents are not sensitive to d_0 and M_0. Figure B1 shows the densities of pseudocomponents for two C_{7^+} fractions with the same average molecular weight and variance as well as average density ($\bar{d} = 0.96$ g/mL, $\bar{M} = 253$ g/mol, and variance $= 700$), but different minimum densities and molecular weights; the first uses $d_0 = 0.70$ g/mL, $M_0 = 84$ g/mol (they correspond to the average values for typical C_6 hydrocarbons), and the second uses $d_0 = 0.73$ g/mL, $M_0 = 98.9$ g/mol. For a careful comparison of density distributions for the C_{7^+} fraction, 20 quadrature points are used in Figure B1. The densities of pseudocomponents are essentially identical for the two sets of d_0 and M_0.

In general, the density of a C_{7^+} pseudocomponent is much larger than that of a normal alkane of the same molecular weight because a C_{7^+} psuedocomponent usually has higher aromaticity. For VLE calculations, we estimate the critical properties of a pseudocomponent from its ambient-condition density and molecular weight using Twu's correlation (1984), and the acentric factor from Lee-Kesler's correlation of acentric factor with critical temperature and normal boiling point (Reid et al., 1986). We expect that these critical properties are more reliable than those obtained using only molecular weight.

Manuscript received Jan 22, 1999, and revision received Aug. 2, 1999.